LAWRENCE
LIVERMORE
NATIONAL
LABORATORY

UCRL-CONF-231791

Fiber-Based, Spatially and Temporally Shaped Picosecond UV Laser for Advanced RF Gun Applications

M. Y. Shverdin, S. G. Anderson, S. M. Betts, D. J. Gibson, F. V. Hartemann, J. E. Hernandez, M. Johnson, I. Jovanovic, M. Messerly, J. Pruet, A. M. Tremaine, D. P. McNabb, C. W. Siders, C. P. J. Barty

June 14, 2007

Particle Accelerator Conference '07
Albuquerque, NM, United States
June 24, 2007 through June 30, 2007

Disclaimer

This document was prepared as an account of work sponsored by an agency of the United States Government. Neither the United States Government nor the University of California nor any of their employees, makes any warranty, express or implied, or assumes any legal liability or responsibility for the accuracy, completeness, or usefulness of any information, apparatus, product, or process disclosed, or represents that its use would not infringe privately owned rights. Reference herein to any specific commercial product, process, or service by trade name, trademark, manufacturer, or otherwise, does not necessarily constitute or imply its endorsement, recommendation, or favoring by the United States Government or the University of California. The views and opinions of authors expressed herein do not necessarily state or reflect those of the United States Government or the University of California, and shall not be used for advertising or product endorsement purposes.

Fiber-Based, Spatially and Temporally Shaped Picosecond UV Laser for Advanced RF Gun Applications*

M. Y. Shverdin†, S. G. Anderson, S. M. Betts, D. J. Gibson, F. V. Hartemann,
J. E. Hernandez, M. Johnson, I. Jovanovic, D. P. McNabb, M. Messerly, J. Pruet, A. M. Tremaine,
C. W. Siders, C. P. J. Barty, Lawrence Livermore National Laboratory, Livermore, CA 94550, USA

Abstract

The fiber-based, spatially and temporally shaped, picosecond UV laser system described here has been specifically designed for advanced rf gun applications, with a special emphasis on the production of high-brightness electron beams for free-electron lasers and Compton scattering light sources. The laser pulse can be shaped to a flat-top in both space and time with a duration of 10 ps at full width of half-maximum (FWHM) and rise and fall times under 1 ps. The expected pulse energy is 50 μJ at 261.75 nm and the spot size diameter of the beam at the photocathode is 2 mm. A fiber oscillator and amplifier system generates a chirped pump pulse at 1047 nm; stretching is achieved in a chirped fiber Bragg grating. A single multi-layer dielectric grating based compressor recompresses the input pulse to 250 fs FWHM and a two stage harmonic converter frequency quadruples the beam. Temporal shaping is achieved with a Michelson-based ultrafast pulse stacking device with nearly 100% throughput. Spatial shaping is achieved by truncating the beam at the 20% energy level with an iris and relay-imaging the resulting beam profile onto the photocathode. The integration of the system, as well as preliminary laser measurements will be presented.

PHOTO-INJECTOR LASER

An energetic, spatially and temporally shaped UV laser system is essential for achieving low emittance, high bright electron beam from an rf gun. At Lawrence Livermore National Lab, this laser system has been built specifically for a Compton-scattering based high brightness gamma-ray source [1]. The laser system provides synchronization of the rf gun photocathode to generate the electron bunches that are accelerated in the S-band linac.

The laser system, shown in Fig. 1 has been designed to deliver "beer-can" (flattop in both space and time) shaped pulses at per pulse energy of 50 μJ at 261.75 nm with very low pulse jitter, high spatial beam quality, stable and robust operation, and simple operation. The laser system consists of a fiber oscillator, fiber-based pulse stretcher and fiber amplification chain which produces a chirped 500 μJ IR pulse at 1047 nm. The IR pulse is then recompressed in a bulk compressor and frequency quadrupled to 261.75 nm. Temporal pulse shaping of the UV pulse occurs in a Hyper-Michaelson interferometer based pulse stacker which reshapes the compressed pulse to a flattop with 10 ps FWHM duration and ≈500 fs fall and rise times [2]. An iris then truncates the beam at the 20% energy level to obtain steep beam boundaries. The truncated beam is then relay-imaged onto a Mg photocathode. We have demonstrated 10^{-4} quantum efficiency with Mg, but 10^{-3} is possible with UV laser cleaning. Simulations predict an electron beam emittance of 1mm.mrad with the designed laser pulse from our photogun [3].

The complete laser system is highly compact; the fiber system fits in two (4'×4'×2') mounted racks and the bulk components occupy one 8'×2' optical breadboard. Key design specifications are summarized in Table 1. The laser system can be scaled to kHz repetition rates.

Table 1: Laser system design specifications

	Fiber Laser	**UV Laser on the RF Gun**
Wavelength (nm)	1047	261.75
Energy (μJ)	500	50
Pulse duration (ps)	5000	10 ps flattop/ 500 fs rise-time
Bandwidth (nm)	8	2-3
Rep rate (Hz)	10	10

Fiber Laser System

A key to building a compact highly stable laser system is a fiber laser front end. A mode-locked and phase-locked fiber oscillator allows sub-picosecond synchronization between the generated electron bunches and the TW-class laser pulses that drive the Compton scattering interaction. The mode-locking mechanism used in this oscillator relies on nonlinear birefringence in a polarization-preserving fiber. The fiber oscillator fits on a 12"×12" breadboard and produces 250 pJ pulses with the bandwidth limited duration of 80 fs at 40.7785 MHz repetition rate. Residual dispersion broadens the pulse to roughly 1 ps and lowers the peak power to 250 W.

The light pulse train produced by the oscillator is stretched for chirped pulse amplification in a corrugated-

*This work was performed under auspices of the U.S. Department of Energy by University of California, Lawrence Livermore National Laboratory under Contract W-7504-Eng-48.

† shverdin2@llnl.gov

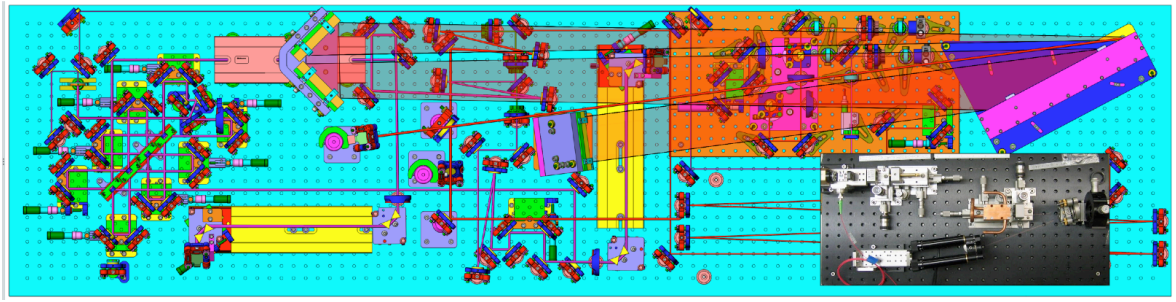

Figure 1: Design of the picosecond laser system. The 8' x 2' breadboard contains the fiber/bulk amplifier, grating compressor, frequency quadrupling crystals and the pulse stacker. The input to the power amplifier is provided by rack mounted fiber oscillator and pre-amplifiers. The output from the laser system is relay imaged onto the photocathode.

fiber Bragg grating stretcher (CFBG) from 1 ps to 5 ns. The stretched pulse is then pre-amplified to 1 μJ in two fiber-based amplifiers, each providing 20 - 30 dB of gain. The final fiber/bulk optic amplifier utilizes a Yb-doped photonic crystal polarizing fiber with a large (41 μm core diameter), boosting the pulse energy from 1 μJ to 500 μJ.

Grating compressor

The compressor compensates for the group delay dispersion (GDD) and 3^{rd}-order dispersion (TOD) introduced in the fiber system, recompressing the input pulse from 5 ns to $\approx$ 250 fs FWHM. The designed compressor is a quad-pass consisting of one 1740 grooves/mm multi-layer dielectric (MLD) grating with a clear aperture of 355$\times$152 mm. The quad-pass compressor achieves a dispersion of 600 ps/nm.

Off-axis beam expander

Resizing of the beam waist at different stages of the laser system is achieved with an off-axis reflective beam (de-) expander [4]. An all reflective design is necessary to eliminate nonlinear phase accumulation that would occur inside the lenses. The beam expander consists of one concave and one convex mirrors placed at a slight angle ($\approx$3 degrees) to each other. This design eliminates astigmatism introduced by a conventional on-axis mirror expander.

Frequency quadrupling

The compressed pulse is frequency-quadrupled from 1047 nm to 261.75 nm. Harmonic conversion occurs in two steps. First, the pulse is frequency-doubled to 523.5 nm with a BBO crystal in Type I configuration (crystal cut angle is 23.2 degrees, crystal thickness is 600 μm). The residual 1047 nm beam is then filtered out using a dichroic mirror. The up-converted beam is then Type I frequency doubled from 523.5 nm to 261.75 nm by a different BBO crystal.

The conversion efficiency from 2ω to 4ω is limited by the 2-photon nonlinear absorption of the UV radiation by the BBO crystal. This constraint is partially overcome by using two 2ω to 4ω doubling crystals. The first BBO crystal partially depletes the green (523.5 nm) pump. The generated UV beam is then separated out with a dichroic mirror. The residual green beam is then sent to a second BBO crystal. The two generated UV beans are later recombined in the hyper-Michelson pulse stacker. The BBO crystals are chosen thin enough to minimize 2-photon absorption. The first 2ω to 4ω BBO crystal is 200 μm thick and the second BBO crystal is 400 μm thick.

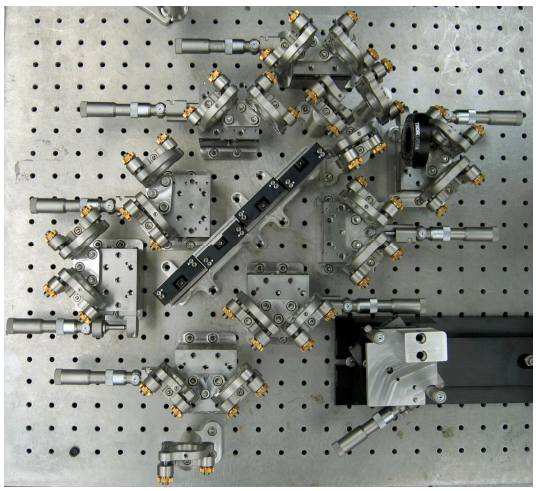

Figure 2: Michelson interferometer based pulse stacker consists of two orthogonally polarized inputs. The output pulse format is set by adjusting the lengths of the interferometer arms. The two inputs are combined at the output on the polarizer.

Pulse stacker

The pulse stacker is a Michelson-based ultrafast pulse multiplexing device having nearly 100% throughput and designed for high energy shaped pulse generation; this system is shown in Fig. 2. The pulse stacker generates a train of replicas of the input pulse delayed with respect to each other with femtosecond precision. Half of the produced pulses are s-polarized and half are p-polarized. Appropriate setting of the interferometer arm lengths can result in

many different output pulse formats. The designed pulse stacker consists of 4 stages and two input ports (for the two generated UV beams), capable of stacking up to 32 pulses. To create the optimal photo-injection pulse, the two UV input pulses are initially temporally stretched to ≈400 fs and then multiplexed with the pulse stacker to create a train of orthogonally polarized pulses spaced by 300 fs, which corresponds to a temporal flattop pulse with 10 ps duration and 500 fs rise-time having some minimal temporal modulation caused by pulse interference (Fig. 3). A prism based pulse stretcher is used to fine adjust the pulse duration prior to sending the pulses through the stacker. To maximize beam throughput and minimize the footprint of the pulse stretcher, we utilize a four-prism set-up. The beam is incident on each of the fused silica prisms at Brewster's angle. A prism pair separation of 50 cm can stretch a 250 fs transform-limited pulse to 1.2 ps FWHM.

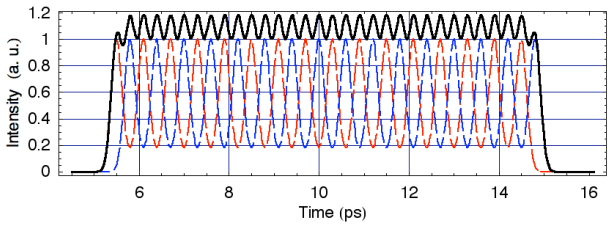

Figure 3: Simulation of the shaped UV pulse after the pulse-stacker. Red and blue dashed lines indicate p and s-polarized pulse trains. The resulting UV pulse on the photocathode is shown by the thick black line. Simulations of the electron beam propagation done in Parmela suggest that the intensity modulation in the resulting laser pulse does not degrade the emittance of the electron bunches.

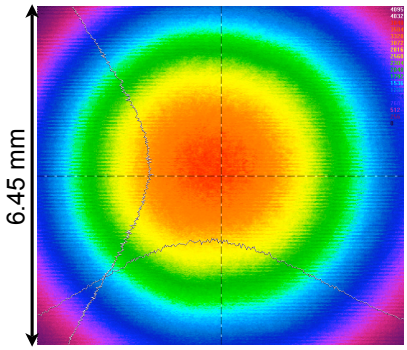

Figure 4: Far-field image of the 1047 nm pulse after the final power amplifier. The image is recorded on the CCD camera after the up-collimated beam after the fiber propagates for 20 m.

Laser diagnostics

The laser system will be fully diagnosed both spatially and temporally. Diagnostics for the laser system, designed to be used while the accelerator is running and therefore remotely operable, will include CCD cameras recording the beam profile at various points (including a virtual cathode image located in the same effective beam plane as the photoinjector cathode) and energy meters and photodiodes recording the laser energy at various points. In addition, a scanning cross-correlator will mix a small sample of the compressed IR light with the stretched, stacked 4ω light in a nonlinear crystal to generate 3ω light to give us a good measure of the temporal properties of the pulse illuminating the photocathode with 200 fs resolution. When the accelerator is not running, a scanning second-order autocorrelator can be used to make routine measurements of the performance of the PDL laser source after the compressor, and it can be used in conjunction with a spectrometer to perform frequency-resolved optical gating (FROG) measurements of the pulse when more detail is needed [5].

RESULTS

The laser system has been assembled and is currently in the process of being optimized. The fiber system has so far achieved an output of 200 μJ at 1047 nm with excellent spatial beam quality (Fig. 4). We anticipate reaching the 500 μJ target shortly. The compressibility of the generated pulse is being examined by sending the pulse after the fiber system through the compressor and performing auto-correlation and FROG measurements. Initial autocorrelation measurements indicate 800 fs FWHM time duration with approximately 50% of the energy contained in the central peak.

Simulations suggest that the observed pre and post pulses will be suppressed in the up-converted 4ω pulse. We are working at improving pulse contrast and decreasing the pulse duration. We anticipate commissioning the laser system within the next several months.

REFERENCES

[1] F.V. Hartemann, W.J. Brown, D.J. Gibson, S.G. Anderson, A.M. Tremaine, P.T. Springer, A.J. Wootton, E.P. Hartouni, and C.P.J. Barty, "High-energy scaling of Compton scattering light sources," Phys. Rev. STAB 8 (2005) 100702.

[2] C. W. Siders, J. L. W. Siders, A. J. Taylor, S.-G. Park, and A. M. Weiner, "Efficient high-energy pulse-train generation using a 2n-pulse Michelson interferometer," Appl. Opt. 37 (1998) 5302.

[3] M. Ferrario, J. E. Clendenin, D. T. Palmer, J. B. Rosenzweig and L. Serafini, HOMDYN study for the LCLS rf photoinjector, The Physics of High Brightness Beams, World Scientific (2000), 534.

[4] P. Hello and C. N. Man, "Design of a low-loss off-axis beam expander," Appl. Opt. 35 (1996) 2534.

[5] R. Trebino, K. W.DeLong, D. N.Fittinghoff, J. N.Sweetser, M. A.Krumbugel, and D. J.Kane, "Measuring ultrashort laser pulses in the time-frequency domain using frequency-resolved optical gating, Rev. Sci. Instrum. 68 (1997) 3277.